

Article

An Application of the Eigenproblem for Biochemical Similarity

Dan-Marian Joița ^{1,*} , Mihaela Aurelia Tomescu ², Donatella Bălint ¹  and Lorentz Jäntschi ^{1,3,*} 

¹ Chemistry Doctoral School, Babeş-Bolyai University, 400084 Cluj, Romania; balintdonna@gmail.com or donatella.balint@ubbcluj.ro

² Department of Mathematics and Informatics, University of Petroşani, 332006 Hunedoara, Romania; MihaelaTomescu@upet.ro

³ Department of Physics and Chemistry, Technical University of Cluj-Napoca, 400641 Cluj, Romania

* Correspondence: djoita@chem.ubbcluj.ro (D.-M.J.); lorentz.jantschi@chem.utcluj.ro (L.J.)

Abstract: Protein alignment finds its application in refining results of sequence alignment and understanding protein function. A previous study aligned single molecules, making use of the minimization of sums of the squares of eigenvalues, obtained for the antisymmetric Cartesian coordinate distance matrices D_x and D_y . This is used in our program to search for similarities between amino acids by comparing the sums of the squares of eigenvalues associated with the D_x , D_y , and D_z distance matrices. These matrices are obtained by removing atoms that could lead to low similarity. Candidates are aligned, and trilateration is used to attach all previously striped atoms. A TM-score is the scoring function that chooses the best alignment from supplied candidates. Twenty essential amino acids that take many forms in nature are selected for comparison. The correct alignment is taken into account most of the time by the alignment algorithm. It was numerically detected by the TM-score 70% of the time, on average, and 15% more cases with close scores can be easily distinguished by human observation.

Keywords: eigenproblem; eigenvalues; molecular alignment; orthogonal alignment; biochemical similarity; antisymmetric matrix



Citation: Joița, D.-M.; Tomescu, M.A.; Bălint, D.; Jäntschi, L. An Application of the Eigenproblem for Biochemical Similarity. *Symmetry* **2021**, *13*, 1849. <https://doi.org/10.3390/sym13101849>

Academic Editors: Anthony Harriman and Enrico Bodo

Received: 13 August 2021
Accepted: 23 September 2021
Published: 2 October 2021

Publisher's Note: MDPI stays neutral with regard to jurisdictional claims in published maps and institutional affiliations.



Copyright: © 2021 by the authors. Licensee MDPI, Basel, Switzerland. This article is an open access article distributed under the terms and conditions of the Creative Commons Attribution (CC BY) license (<https://creativecommons.org/licenses/by/4.0/>).

1. Introduction

Just visualizing two simple similar structures leads to an immediate detection of patterns. Similarity is of convenience for humans, but to power automatic decision mechanisms for a PC, it must be measurable. It is mostly used for comparing proteins, but the growing number of PDB structures (currently over 180,000) is many orders of magnitude higher than what the human eye can compare. Because of the large number, it takes days even for current programs to search the database for a query structure. A more reasonable time can be achieved by developing new algorithms [1].

Protein alignment finds its application in refining results of sequence alignment and understanding protein function [2,3]. Choosing the alignment that is most geometrically similar is an easier task compared to evaluating its biological significance [4]. The pursuit of the best method is in progress, with multiple programs being developed during the past decades:

- CAB-Align uses the residue–residue contact area to identify regions of similarity [5].
- Caretta uses rotation-invariant technique signals of distances derived from overlapping contiguous stretches of residues to find an initial superposition [6].
- DALI [7].
- LS-align generates fast and accurate atom-level structural alignments of ligand molecules through an iterative heuristic search of the target function that combines comparisons of inter-atom distance with mass and chemical bonds [8].
- MATT uses a fragment-based approach that allows for local flexibility between fragment pairs from two input structures and then a dynamic programming algorithm to assemble these intermediate pairs [9].

- TM-align uses the length-independent TM-score as a measure of similarity between two proteins in a dynamic programming approach [10].

Some advances have been made in relation to these algorithms, such as parallel re-implementation of mTM-align/TM-align pm-TM-align [11], parMATT [12], heuristic algorithms, and hierarchical organization mTM-align [13].

The 3D variant of the distance matrix alignment method (DALI) uses rotation and translation in order to achieve a smaller distance between equivalent points in the two molecules [14].

In a previous study, the eigenproblem was employed to achieve the proper alignment of single molecules, or the mirror of the proper alignment, and this can be exploited to reduce the number of rotations for which a scoring function needs to run [15].

The eigenproblem is thus defined in the literature as follows:

Given the quadratic matrix A , of the order n , $\lambda \in \mathbb{C}$ is called the eigenvalue of the matrix A and $X \neq 0$ its associated eigenvector if the relationship $AX = \lambda X$ is satisfied. The matrix $\lambda I - A$ is singular (because $\det(\lambda I - A) = 0$), where I is the unit matrix of the order n . The solutions of the equation $\det(\lambda I - A) = 0$ represent the eigenvalues of the matrix A .

The determinant $\det(\lambda I - A)$ is called the characteristic polynomial (ChP) associated with the matrix A . It has a degree equal to the order of the matrix so that the eigenvalues of the matrix A are its roots.

The eigenproblem in relation to geometrical alignment was stated before in the context of surface analysis [16] and control and can go in another direction in the context of amino acids. A subject of the study is a solution to the eigenproblem of amino acid alignment. The Cartesian system is rotated and eventually translated and reflected until the structure arrives at a position characterized by the highest absolute values of the eigenvalues observed on the Cartesian coordinates.

The aim of this study is to find the best geometric alignment of 20 selected amino acids with regard to each other. An extension to the previous study described by Jäntschi [15] has been elaborated. Sums of the squares of eigenvalues ($S_T = -2S_x - 2S_y - 2S_z$) for all three Cartesian coordinate distance matrices (D_x , D_y , and D_z) are compared. By removing atoms, smaller D_x , D_y , and D_z matrices are obtained and more S_T sums are added to the comparison. Percentual similarities are found between these sums. Candidates are aligned by the eigenproblem algorithm, and trilateration is used to attach all previously striped atoms. To verify, a TM-score is run on the resulting full-structure candidates.

2. Materials and Methods

In [15], it was shown that the Cartesian distance matrix is antisymmetric and therefore its eigenvalues are purely imaginary, as well as the fact that the best alignment of a molecule is obtained for the minimum value of the sum of the squares of eigenvalues of the Cartesian distance matrix.

Thus, the angle of rotation of the structure must be found around an axis for which the minimum of this amount is obtained. One method of finding the angle of rotation around an axis for the best alignment is as follows: in the case of an amino acid with 5 atoms, we note the vertices of the graph corresponding to the organic compound with $V_i(x_i, y_i, z_i)$, $i = \overline{1, 5}$. We want to find the optimal angle of rotation around the Oz axis, for example. The

characteristic polynomial associated with the matrix of Cartesian distances on Ox can be approximated in this way:

$$\text{ChP}(\lambda, Dx) = \lambda^3 \left[\lambda^2 + \sum_{\substack{j = \overline{1,4} \\ i = \overline{2,5} \\ j < i}} (x_i - x_j)^2 \right], \quad (1)$$

which leads to the problem of finding the rotation angle in the xOy plane so as to obtain the maximum value of the sum

$$S_x = \sum_{\substack{j = \overline{1,4} \\ i = \overline{2,5} \\ j < i}} (x_i - x_j)^2. \quad (2)$$

Because the term $(x_i - x_j)^2$ becomes maximum when $\sphericalangle(V_j V_i, Ox) = 0$, we calculate the amount S_x using the law of motion of the rotation of a body about a fixed axis:

$$\begin{cases} x'_i = x_i \cos \varphi - y_i \sin \varphi \\ y'_i = x_i \sin \varphi + y_i \cos \varphi \end{cases}$$

where φ , in turn, takes the value $\sphericalangle(V_j V_i, Ox)$; $j = \overline{1,4}$; $i = \overline{2,5}$; $j < i$.

Using the interpolation method, we find the value of the angle of rotation around the Oz axis. Similarly, we proceed to find the angle of rotation of the structure around one of the other two axes.

The eigenvalues of the associated Cartesian coordinate distance matrix Dx are always two conjugate purely imaginary solutions: $\lambda_1^2 = \lambda_2^2 = -S_x$. Sums of the form $S_T = -2S_x - 2S_y - 2S_z$, associated with Dx, Dy, and Dz matrices, are compared in order to find similarities.

Starting from the eigenproblem approach, 20 essential amino acids that take many forms in nature are selected from available databases.

The alignments for these amino acids (downloaded from PubChem), with compound CIDs 750, 5862, 5950, 5951, 5960, 5961, 5962, 6057, 6106, 6137, 6140, 6267, 6274, 6287, 6288, 6305, 6306, 6322, 33032, 145742, are computed. In this example, the one with the fewest heavy atoms is chosen for reference, glycine 00750.sdf. The following tables for the other cases in which the rest of the structures are references can be found in the Supplementary Materials section:

- 3D structural data for heavy atoms
- 3D distance matrix for heavy atoms

Tables 1–3 depict the Cartesian coordinate distance matrices for heavy atoms. They are antisymmetric, so their eigenvalues, in Table 4, are imaginary.

Table 1. First Cartesian coordinate (x) distance matrix for glycine (heavy atoms).

Dx	1	2	3	4	5
1	0	0.010	0.001	0.018	0.022
2	−0.010	0	−0.008	0.008	0.013
3	−0.001	0.008	0	0.017	0.021
4	−0.018	−0.008	−0.017	0	0.004
5	−0.022	−0.013	−0.021	−0.004	0

Table 2. Second Cartesian coordinate (y) distance matrix for glycine (heavy atoms).

Dy	1	2	3	4	5
1	0	1.951	0.738	−0.130	0.726
2	−1.951	0	−1.212	−2.080	−1.224
3	−0.738	1.212	0	−0.868	−0.012
4	0.130	2.080	0.868	0	0.856
5	−0.726	1.224	0.012	−0.856	0

Table 3. Third Cartesian coordinate (z) distance matrix for glycine (heavy atoms).

Dz	1	2	3	4	5
1	0	−1.165	−3.549	−2.383	−1.146
2	1.165	0	−2.384	−1.218	0.019
3	3.549	2.384	0	1.166	2.403
4	2.383	1.218	−1.166	0	1.236
5	1.146	−0.019	−2.403	−1.236	0

Table 4. Eigenvalues for glycine (heavy atoms).

	x ₁	x ₂	x ₃	x ₄	x ₅
[Dx]	6.065i	−6.065i	0	0	0
[Dy]	3.698i	−3.698i	0	0	0
[Dz]	0.044i	−0.044i	0	0	0

It can be observed that unlike eigenvalues for a symmetric matrix, we obtain a single pair of complementary imaginary numbers regardless of the number of atoms in the compound. Another good part of this approach is that, as shown in Table 5, the polynomial can be expressed with real-value coefficients as a product of a polynomial of degree 2 and a monomial of degree (n − 2), leading to a faster response from the program.

Table 5. The polynomials of [Dx], [Dy], and [Dz] for glycine (heavy atoms).

Matrix (A)	$ \lambda \cdot \mathbf{I} - \mathbf{A} $ Polynomial
[Dx]	$\lambda^3 \cdot (\lambda^2 + 36.7783)$
[Dy]	$\lambda^3 \cdot (\lambda^2 + 13.6746)$
[Dz]	$\lambda^3 \cdot (\lambda^2 + 0.0019791)$

Making use of the eigenproblem approach (named the OrigEig function), the other amino acids are aligned to glycine. Candidates with a lower number of atoms than the original are processed while searching for S_T similarities. The rest of the atoms are later added using a trilateration algorithm found and used from the literature [17]. Some capabilities are added, such as importing original data (*.sdf or *.xyz by the impCart function); performing *.sdf to *.xyz file conversion; removing hydrogen atoms for convenience; and exporting all compared rotated structures as *.xyz (by the writexyz function), a scoring function based on the TM-score and the creation of *.xls files. The code and its explanation can be found in the Supplementary Materials section, and a schematic overview is available in Figure 1.

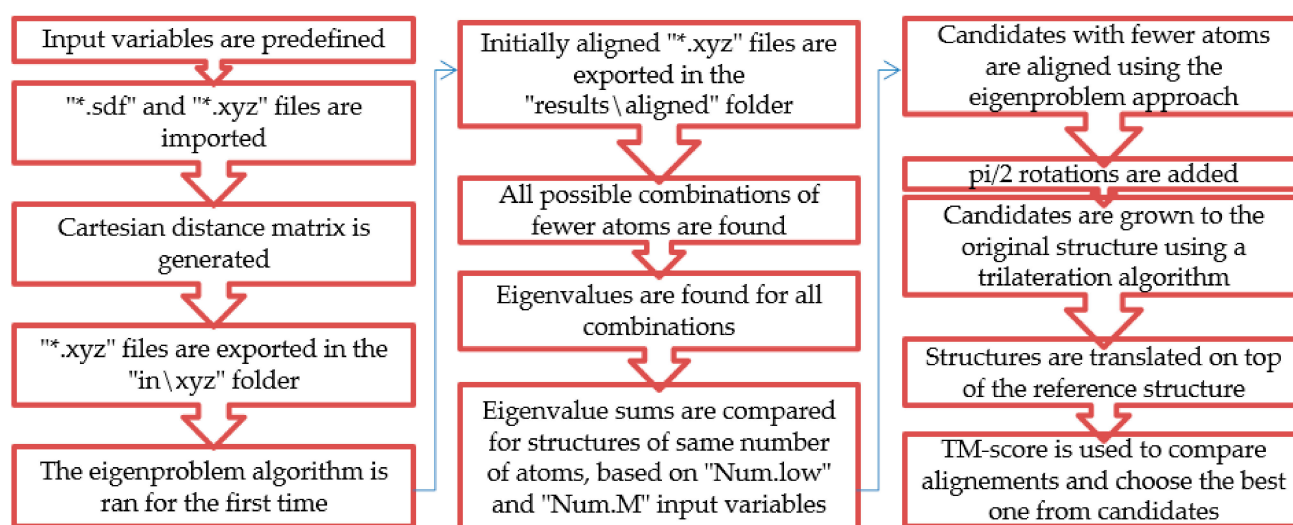


Figure 1. A schematic overview of the algorithm.

The requirements for this application are:

- The “in” and “results” directories, the former containing an “xyz” directory and the latter containing “aligned,” “rotated,” and “tables” directories
- Geometrically optimized amino acid *.xyz or *.sdf files that need to be located in the “in” folder
- The name of the file representing the selected reference amino acid or the number associated with the file (1 representing the first file in the “in” directory)
- Input variable Num.M, which defines how many extra candidates can be taken into consideration in case Num.low is satisfied by only one candidate
- Input variable Num.low, which defines the target percentage differences between S_T of two candidates in order to accept and stop searching for candidates with fewer atoms
- Input variable Num.low2, which defines the percentage of the maximum found TM-score such that even lower-scored candidates are exported in *.xls tables and *.xyz files
- Input variables Num.empi1 through 3 needed by the TM-score or another means of choosing between alignments

After the requirements are met, the original eigenproblem algorithm is run in order to be sure that the starting point of the program is a good initial alignment. Then all possible combinations with a smaller number of atoms are found by eliminating atom by atom in the ALLIE function. Eigenvalues are found for each combination without rotating the candidates. S_T sums are compared until the input variables are satisfied or all combinations with a minimum of three atoms are compared. Candidates are aligned by the original eigenproblem approach, possibly good $\pi/2$ rotations are taken into consideration, and trilateration is run. Since the TM-score compares distances between atoms of molecules, candidates are translated on top of the reference structure. Good final candidates are exported.

The following tables are exported as *.xls files in the “results\tables” directory:

1. 3D structural data for heavy atoms as T1
2. 3D distance matrix for heavy atoms as T2
3. Cartesian coordinate distance matrices for heavy atoms as T3–T5
4. Eigenvalues for above Cartesian coordinate distance matrices as T6
5. Polynomials for the same Cartesian coordinate distance matrices as T7
6. A table containing data such as Table A1 available in Appendix A, but no images, named Tscore

The following files are exported as *.xyz geometry files:

- Initial *.sdf files are converted in the “in\xyz” directory.

- In the “results\aligned” directory, the results from the original eigenproblem program are exported.
- In the “results\rotated” directory, all *.xyz files related to the Tscore table can be found.

3. Results

Eigenvalues of all combinations of atoms are computed for each structure. The $-2S_x$, $-2S_y$, and $-2S_z$ values of Dx, Dy, and Dz matrices for aligned glycine are -73.557 , -27.349 , and -0.004 , respectively; sum $S_T = -100.91$.

Comparing alanine 005950.sdf to glycine, six possible combinations of five atoms can be found, the fifth having the closest sum to -100.91 , as seen in Table 6.

Table 6. All combinations of five atoms in the case of alanine and their S_T sums.

	Possible Atom Choices						S_T
1	O2	N3	C4	C5	C6	-103.395	
2	O1	N3	C4	C5	C6	-107.168	
3	O1	O2	C4	C5	C6	-102.657	
4	O1	O2	N3	C5	C6	-134.779	
5	O1	O2	N3	C4	C6	-101.514	
6	O1	O2	N3	C4	C5	-136.012	

All possible candidates are parsed by the moreData function in the search for a lower percentage difference between S_T sums (in the indx function). The targeted percentage difference is defined by Num.low. A multiplier is chosen to extend the search range at the cost of time, Num.M, since the best alignment might not necessarily be the one with the lowest difference between sums. In this case, the following three are chosen by the program: 1, 3, and 5.

The eigenproblem approach is used on the chosen candidates to obtain an eigenvalue-wise rotation alignment. It is suggested that compounds are obtained in their correct alignment or in the mirror of the proper alignment [15]. The search is extended to these possible good rotations (by the first “for” instruction of the align function). To obtain the position of the other unmatched unaligned atoms, a trilateration algorithm (receiving data from the rest of the align function) is found and used from the literature [17].

Since one of these rotations should lead to a good superposition of the two amino acids, the mean values on each of the axes are found for selected atoms of both structures. The selection is based on atoms indexed in the candidate search presented in Table 6. Subtracting for each of the axes, the candidate structure is translated on top of glycine (by the trans function).

For the resulting candidate combinations, distances are found between pairs of a number of atoms. A MATLAB function matchpairs is used to find atoms that will be superposed based on a linear assignment problem that allows for minimum-cost solutions. These pairs are introduced into a scoring function chosen from the literature, in this case the geometric part of UniAlign-TMscore [2]. All these are executed by the choice function. One change was made since our chosen structures contain a small number of atoms: the 15 subtraction was set to 0 so that we obtained a positive distance under the square root of the empirical scaling factor for distance normalization, d0. This can be modified in empi3. Other scoring functions may be applied. The best result for alanine is superposed in Figure 2 in tube style, on top of glycine, which is presented in ball-and-stick-with-non-colored-bond style.

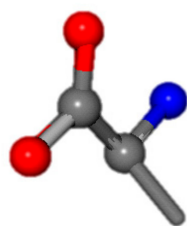


Figure 2. A 3D view of the best alignment of alanine to glycine.

The best score for each compared structure is exported to the final results in Table A1 available in Appendix A. Using another parameter (Num.low2), scores close to it are added. Elements selected for candidates with fewer atoms are presented in the table since they help make an easy choice between close scores. A *Tscore.xls file is generated at the end of the choice function.

4. Discussion

The TM-score can be used to select a best match from all candidates found by the eigenproblem algorithm, as seen in Tables A1 and A2 of Appendix A. Of the total of 19 amino acids aligned to glycine, 13 results are singular high-confidence alignments, of which 11 give a high TM-score. Another three (cysteine, lysine, and arginine) give two possible good results each, and the TM-score can be used to distinguish the best one.

There are some mismatches made by the program. For example, in the case of glutamine 005961, the best score is found for a four-atom alignment instead of the correct five-atom alignment case number 483. Another difficulty can be observed in the cases of tryptophan 006305 and glutamic acid 033032, where a small score is given to the aligned case numbers 4/115, which are the only ones with elemental similarities, as depicted in Table 7.

Cysteine is the second amino acid taken as a reference for alignment, and all the candidates that our program outputs are depicted in Table A2 of Appendix A. From the total of 19 amino acids aligned to cysteine, six results can be chosen by the highest TM-score, of which two are singular results. Another five give two or more possible good results each, and the TM-score can be used to distinguish the best one.

The following eight mismatches are presented for cysteine, of which the first four are available in Table 8:

- In the case of alanine 005950, a small score is given to the aligned case number 269, which is the only one with elemental similarity.
- For valine 006287, threonine 006288, and arginine 006322, the best scores are found for candidates with a lower number of aligned atoms. The best candidates with more aligned atoms are 006287-1, 006288-1, and 6322-19.
- The outputs for aspartic acid 005960, lysine 005962, histidine 006274, and tryptophan 006305 did not contain the expected alignments.

As stated above, a parameter is introduced such that close scores are not ignored. In this case, a score of 80% of the maximum is accepted for output. This percentage can be indicated in the Num.low2 parameter. This is needed so that the best alignment is given as a result, even though it is not the one with the highest TM-score.

Another easy way to choose from these candidates is to view the chosen elements and eliminate candidates that might have close numerical scores but wrong atom types. Other scoring functions or a combination of such means could lead to even better results.

Table 7. 3D views of the problematic choice of alignments for glycine.

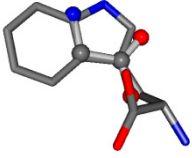
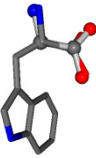
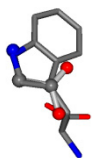
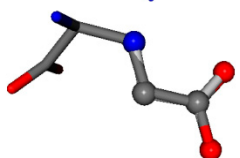
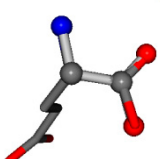
3D Views of Alignment	Aligned Structure and Index	TM-Score	Selected Atoms from 000750	Selected Atoms from the Aligned Structure
	006305-1	0.80948	OONCC	CCCCC
	006305-4	0.66756	OONCC	OONCC
	006305-42	0.7386	OONCC	CCNCC
	033032-69	0.96492	OONCC	OOCCC
	033032-115	0.93477	OONCC	OONCC

Table 8. 3D views of the problematic choice of alignments for cysteine.

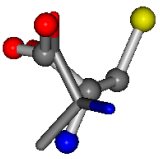
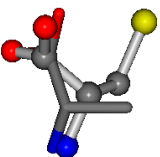
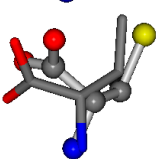
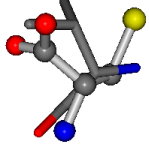
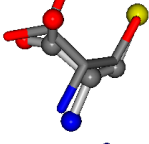
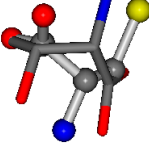
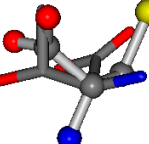
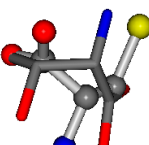
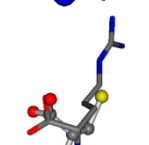
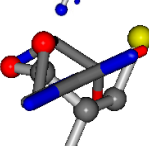
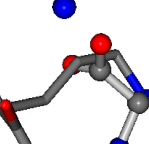
3D Views of Alignment	Aligned Structure and Index	TM-Score	Selected Atoms from 000750	Selected Atoms from the Aligned Structure
	005950-248	0.60276	OONCC	OOCCC
	005950-269	0.56223	OONCC	OONCC
	006287-1	0.44763	SOONCCC	COONCCC

Table 8. Cont.

3D Views of Alignment	Aligned Structure and Index	TM-Score	Selected Atoms from 000750	Selected Atoms from the Aligned Structure
	006287-10	0.50113	ONCCC	COCNC
	006288-1	0.48391	SOONCCC	OOONCCC
	006288-13	0.51827	SONCCC	NCOCCC
	006288-26	0.5201	SOOCCC	OCOCCC
	006288-28	0.51827	SONCCC	NCOCCC
	006322-19	0.4956	SOONCCC	COONCCC
	006322-42	0.5614	SOOCCC	OCNCOC
	006322-69	0.51145	SOOCCC	NCCNCC

The use and applicability of the eigenproblem goes beyond the alignment of molecules [15] and biochemical similarity. Recent reports include analysis of regular graphs for their properties, including eigen-spectra and automorphisms [18], molecular topology [19–22], characteristic equations, principal component decomposition [23], algebraic topology and generalized Bertrand curves [24], treatment of fuzzy decisions [25] and tridiagonal matrices [26], commutator tables, and Laplacian [27], systems of differential [28], and integro-differential [29] equations, while challenging problems appear in polynomial root evaluation [30] and the characteristic equation of a square matrix of a great order [31].

5. Conclusions

An application of the eigenproblem was elaborated, aiming to find the best geometric alignment of selected amino acids with regard to each other.

We can conclude that the best alignment does not obey a strict trend. The close results of the same algorithm can be taken into account. Even after running a score function, we can conclude that the alignment with the highest score is not always the best alignment.

To reduce the number of rotations for which a scoring function is run, the present algorithm needs to be restricted with a few parameters. In addition, a combination of multiple approaches could lead to faster results.

Taking glycine as a reference, 84% of the best alignments can be numerically pointed by a scoring function such as the TM-score, of which 68% are exported as single candidates, meaning that the restrictive parameters are relevant to the present comparison. For cysteine, only 58% can benefit from the presented scoring function. An extensive database would reveal a logical way of choosing them and help training for machine learning.

After running the present algorithm with the other amino acids as a reference, the correct alignment was numerically detected by the TM-score 70% of the time, on average, and 15% more cases with close scores can be easily distinguished by human observation. The present algorithm can be sped up by full vectorization. Machine learning needs to be added to scoring functions as a means to reduce the impact of limited description capabilities and predetermined theory-inspired functional form. These shortcomings can be solved by not imposing a strict algorithm but letting machine learning capture properties that are hard to model because of many unmeasured/unknown/undiscovered quantitative structure–activity relationships (QSAR). Machine learning can assimilate the fast-growing volume of high-quality structural and interaction data found in the literature.

Supplementary Materials: The following archive is available online at <https://www.mdpi.com/article/10.3390/sym13101849/s1>: *.zip archive, containing results in *.xyz format, *.xls tables, and pictures of a 3D view of alignments for each amino acid taken as a reference.

Author Contributions: Conceptualization, L.J.; software, L.J. and D.-M.J.; data curation, D.B.; writing, D.-M.J. and M.A.T.; supervision, L.J. All authors have read and agreed to the published version of the manuscript.

Funding: The present work received financial support through the project “Entrepreneurship for Innovation through Doctoral and Postdoctoral Research,” POCU/380/6/13/123886, co-financed by the European Social Fund, through the Operational Program for Human Capital 2014-2020. This research was funded by the Technical University of Cluj-Napoca open access publication grant.

Institutional Review Board Statement: Not applicable.

Informed Consent Statement: Not applicable.

Data Availability Statement: The data presented in this study are available in the *.zip archive of the Supplementary Materials section of this article.

Conflicts of Interest: The authors declare no conflict of interest.

Appendix A

Aligned amino acids are superposed in Table A1 in tube style on top of glycine, which is presented in ball-and-stick-with-non-colored-bond style. Each amino acid is taken as a reference and presented in its own *Tscore.xls file in the Supplementary Materials section. Three-dimensional renders can be found in the pictures folders of the archive.

Table A1. All structures aligned to glycine; their candidate indexes as exported by the program in *.xyz format; TM-scores; selected elements; and $-2S_x$, $-2S_y$, and $-2S_z$.

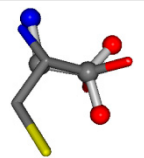
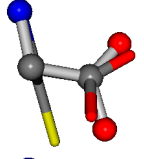
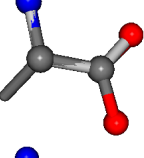
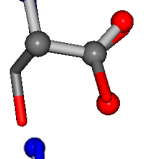
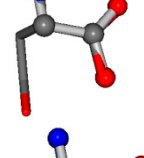
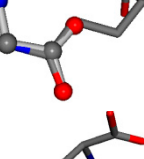
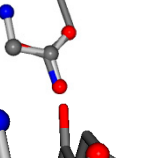
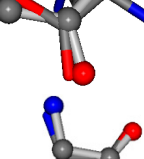
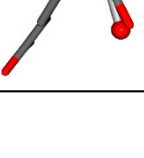
3D Views of Alignment	Aligned Structure and Index	TM-Score	Selected Atoms from 000750	$-2S_x$, $-2S_y$, and $-2S_z$ of the Reference Candidate	Selected Atoms from the Aligned Structure	$-2S_x$, $-2S_y$, and $-2S_z$ of the Aligned Candidate
	005862-13	0.49953	OONCC	-0.004 -27.3493 -73.5567	OONCC	-13.611 -25.8092 -61.4329
	005862-14	0.59034	OONCC	-0.004 -27.3493 -73.5567	OONCC	-13.611 -25.8092 -61.4329
	005950-3	0.97619	OONCC	-0.004 -27.3493 -73.5567	OONCC	-4.4817 -70.1638 -28.7497
	005951-41	0.80012	OONCC	-0.004 -27.3493 -73.5567	OONCC	-69.7742 -4.2881 -26.9964
	005960-37	0.86944	OONCC	-0.004 -27.3493 -73.5567	OONCC	-71.2314 -27.4581 -2.0944
	005961-33	0.84632	OONCC	-0.004 -27.3493 -73.5567	OONCC	-71.2576 -3.3832 -27.3196
	005961-170	0.95817	OCC	-0.0011 -20.6582 -23.8791	OCNC	-24.0884 -0.0004 -21.1849
	005961-173	0.93357	OCC	-0.0011 -20.6582 -23.8791	NCOC	-0.0004 -24.0884 -21.1849
	005961-198	0.79095	OCC	-0.0011 -20.6582 -23.8791	OCOC	-0.2581 -24.3734 -20.2611
	005961-283	0.82694	OONCC	-0.0022 -14.8281 -54.3193	OONCC	-53.2066 -1.5086 -15.0372

Table A1. Cont.

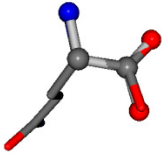
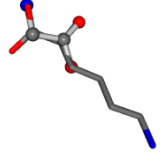
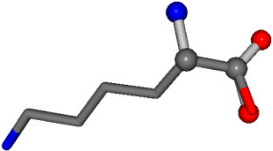
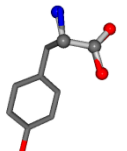
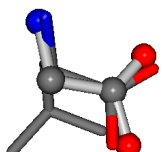
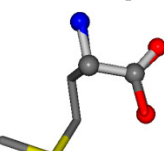
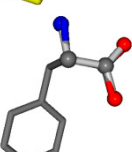
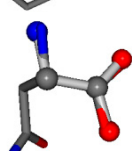
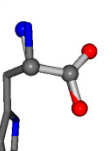
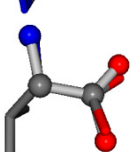
3D Views of Alignment	Aligned Structure and Index	TM-Score	Selected Atoms from 000750	$-2S_{x_r}$, $-2S_{y_r}$, and $-2S_{z_r}$ of the Reference Candidate	Selected Atoms from the Aligned Structure	$-2S_{x_r}$, $-2S_{y_r}$, and $-2S_{z_r}$ of the Aligned Candidate
	005961-483	0.85761	OONCC	-0.0032 -4.3992 -57.2565	OONCC	-54.6736 -2.475 -21.8424
	005962-12	0.75429	OONCC	-0.004 -27.3493 -73.5567	CNOCC	-70.2261 -29.0349 -4.2049
	005962-40	0.91715	OONCC	-0.004 -27.3493 -73.5567	OONCC	-1.5282 -26.4302 -73.3027
	006057-40	0.86353	OONCC	-0.004 -27.3493 -73.5567	OONCC	-2.3691 -27.3223 -70.9619
	006106-2	0.6392	OONCC	-0.004 -27.3493 -73.5567	OONCC	-8.1806 -61.8107 -30.7736
	006137-40	0.86184	OONCC	-0.004 -27.3493 -73.5567	OONCC	-2.2896 -27.3359 -71.1183
	006140-40	0.86912	OONCC	-0.004 -27.3493 -73.5567	OONCC	-2.1499 -27.3655 -71.1355
	006267-2	0.86616	OONCC	-0.004 -27.3493 -73.5567	OONCC	-7.4136 -64.3092 -29.0284
	006274-41	0.83006	OONCC	-0.004 -27.3493 -73.5567	OONCC	-69.8017 -3.9136 -26.9388
	006287-15	0.69499	OONCC	-0.004 -27.3493 -73.5567	OONCC	-68.0382 -8.7019 -24.3289

Table A1. Cont.

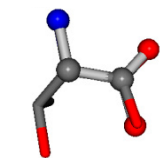
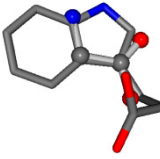
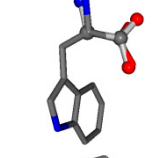
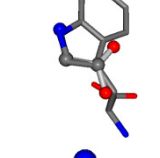
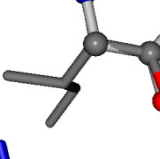
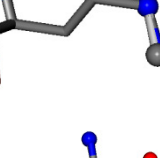
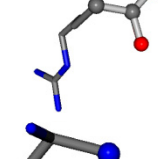
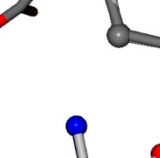
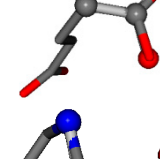
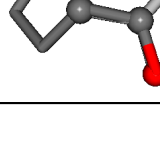
3D Views of Alignment	Aligned Structure and Index	TM-Score	Selected Atoms from 000750	$-2S_{x_r}$, $-2S_{y_r}$, and $-2S_{z_r}$ of the Reference Candidate	Selected Atoms from the Aligned Structure	$-2S_{x_r}$, $-2S_{y_r}$, and $-2S_{z_r}$ of the Aligned Candidate
	006288-65	0.92522	OONCC	-0.004 -27.3493 -73.5567	OONCC	-72.4925 -27.4791 -1.3521
	006305-1	0.80948	OONCC	-0.004 -27.3493 -73.5567	CCCCC	-0.0317 -25.8926 -74.5664
	006305-4	0.66756	OONCC	-0.004 -27.3493 -73.5567	OONCC	-0.0317 -74.5664 -25.8926
	006305-42	0.7386	OONCC	-0.004 -27.3493 -73.5567	CCNCC	-1.1175 -25.7209 -72.1151
	006306-11	0.82228	OONCC	-0.004 -27.3493 -73.5567	OONCC	-70.3452 -26.3299 -4.0766
	006322-14	0.97621	OONCC	-0.004 -27.3493 -73.5567	NNCNC	-73.6395 -27.5846 -0.0063
	006322-93	0.99322	OONCC	-0.004 -27.3493 -73.5567	OONCC	-72.695 -0.0803 -27.8005
	033032-69	0.96492	OONCC	-0.004 -27.3493 -73.5567	OOCCE	-79.1546 -0.3715 -26.9955
	033032-115	0.93477	OONCC	-0.004 -27.3493 -73.5567	OONCC	-73.0115 -27.7341 -1.111
	145742-4	0.92766	OONCC	-0.004 -27.3493 -73.5567	OONCC	-6.2518 -65.5464 -27.6594

Table A2. All structures aligned to cysteine; their candidate indexes as exported by the program in *.xyz format; TM-scores; selected elements; and $-2S_x$, $-2S_y$, and $-2S_z$.

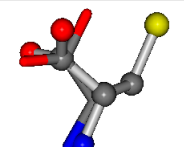
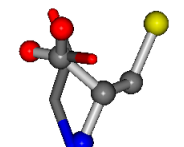
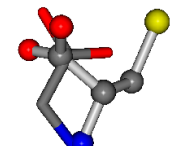
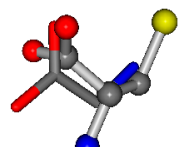
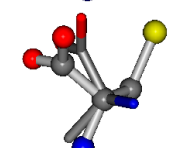
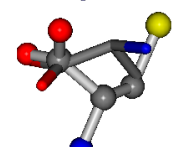
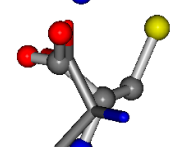
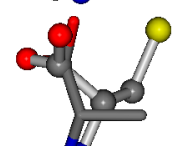
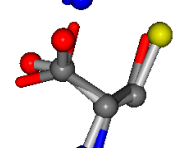
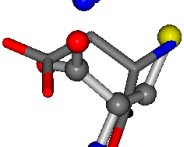
3D Views of Alignment	Aligned Structure and Index	TM-Score	Selected Atoms from 000750	$-2S_x$, $-2S_y$, and $-2S_z$ of the Reference Candidate	Selected Atoms from the Aligned Structure	$-2S_x$, $-2S_y$, and $-2S_z$ of the Aligned Candidate
	000750-6	0.48834	OONCC	-13.611 -25.8092 -61.4329	OONCC	-73.5567 -27.3493 -0.004
	000750-8	0.42207	OONCC	-13.611 -25.8092 -61.4329	OONCC	-73.5567 -0.004 -27.3493
	000750-10	0.44278	ONCCC	-13.611 -25.8092 -61.4329	ONCOC	-0.004 -27.3493 -73.5567
	000750-11	0.44133	OCCC	-13.611 -25.8092 -61.4329	OCNC	-73.5567 -27.3493 -0.004
	005950-148	0.50246	OONCC	-8.3671 -29.9695 -62.0051	OOCCC	-71.7263 -5.4464 -25.4841
	005950-164	0.5433	OOCCC	-8.3671 -29.9695 -62.0051	OOCCC	-71.7263 -25.4841 -5.4464
	005950-248	0.60276	OONCC	-8.3671 -29.9695 -62.0051	OOCCC	-71.7263 -5.4464 -25.4841
	005950-269	0.56223	OONCC	-8.3671 -29.9695 -62.0051	OONCC	-0.31 -73.3751 -27.8286
	005951-16	0.78486	SOONCCC	-37.2279 -107.1892 -159.5151	OOONCCC	-147.0913 -24.8576 -106.5052
	005960-1	0.42025	SOONCCC	-37.2279 -107.1892 -159.5151	NOCOCCC	-11.3045 -110.1124 -182.4483

Table A2. Cont.

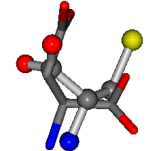
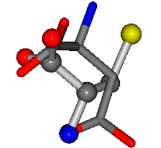
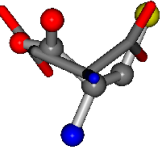
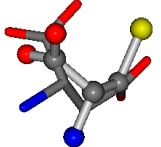
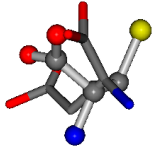
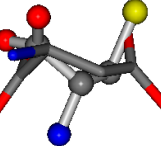
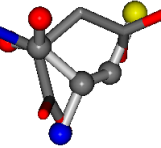
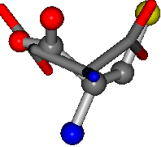
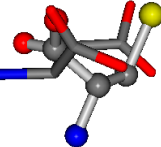
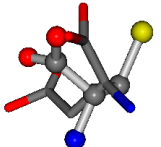
3D Views of Alignment	Aligned Structure and Index	TM-Score	Selected Atoms from 000750	$-2S_x$, $-2S_y$, and $-2S_z$ of the Reference Candidate	Selected Atoms from the Aligned Structure	$-2S_x$, $-2S_y$, and $-2S_z$ of the Aligned Candidate
	005960-6	0.4143	SONCCC	-37.2279 -107.1892 -159.5151	OCNCCC	-11.3045 -182.4483 -110.1124
	005960-7	0.3736	SOONCCC	-37.2279 -107.1892 -159.5151	NOOCCCC	-182.4483 -110.1124 -11.3045
	005960-10	0.42411	SOOCCC	-37.2279 -107.1892 -159.5151	CNCCOC	-11.3045 -182.4483 -110.1124
	005960-12	0.40875	SOONCCC	-37.2279 -107.1892 -159.5151	OOOCCCC	-182.4483 -110.1124 -11.3045
	005960-13	0.39022	OONCC	-37.2279 -107.1892 -159.5151	OCCCC	-110.1124 -11.3045 -182.4483
	005960-14	0.39347	SOONCCC	-37.2279 -107.1892 -159.5151	ONCOCCC	-11.3045 -110.1124 -182.4483
	005960-15	0.45748	SOONCCC	-37.2279 -107.1892 -159.5151	CCNOCOC	-11.3045 -110.1124 -182.4483
	005960-24	0.42411	SOOCCC	-37.2279 -107.1892 -159.5151	CNCCOC	-110.1124 -11.3045 -182.4483
	005960-25	0.37188	SOOCCC	-37.2279 -107.1892 -159.5151	CONCOC	-182.4483 -110.1124 -11.3045
	005960-26	0.39022	OONCC	-37.2279 -107.1892 -159.5151	OCCCC	-11.3045 -110.1124 -182.4483

Table A2. Cont.

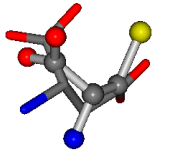
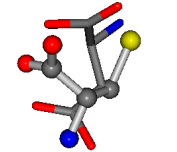
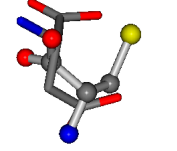
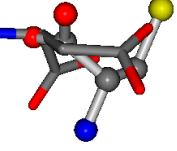
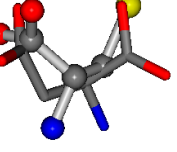
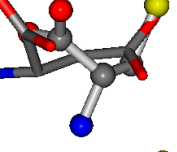
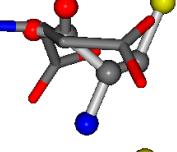
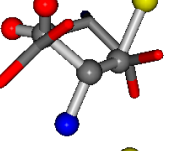
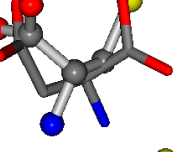
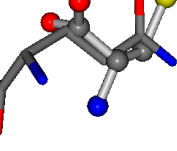
3D Views of Alignment	Aligned Structure and Index	TM-Score	Selected Atoms from 000750	$-2S_x$, $-2S_y$, and $-2S_z$ of the Reference Candidate	Selected Atoms from the Aligned Structure	$-2S_x$, $-2S_y$, and $-2S_z$ of the Aligned Candidate
	005960-27	0.40875	SOONCCC	-37.2279 -107.1892 -159.5151	OOCCCC	-24.9542 -207.716 -70.9892
	005960-28	0.39485	SOONCCC	-37.2279 -107.1892 -159.5151	NOOCCCC	-207.716 -24.9542 -70.9892
	005960-31	0.3717	SOONCCC	-37.2279 -107.1892 -159.5151	OCCOCOC	-24.9542 -207.716 -70.9892
	005960-35	0.42601	SOCCC	-37.2279 -107.1892 -159.5151	OCCOC	-24.9542 -207.716 -70.9892
	005960-37	0.42553	SOONCCC	-37.2279 -107.1892 -159.5151	OOCCCC	-207.716 -70.9892 -24.9542
	005960-43	0.43719	SOOCCC	-37.2279 -107.1892 -159.5151	OOCOCC	-207.716 -70.9892 -24.9542
	005960-49	0.42601	SOCCC	-37.2279 -107.1892 -159.5151	OCCOC	-70.9892 -24.9542 -207.716
	005960-50	0.46341	SOOCCC	-37.2279 -107.1892 -159.5151	COCOCC	-207.716 -70.9892 -24.9542
	005960-52	0.42553	SOONCCC	-37.2279 -107.1892 -159.5151	OOCCCC	-207.716 -70.9892 -24.9542
	005961-14	0.61685	SCCC	-31.8416 -89.3906 -126.7171	OCCC	-1.4071 -33.3867 -210.7718

Table A2. Cont.

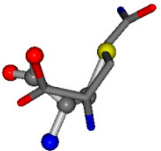
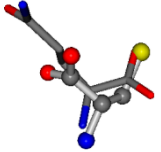
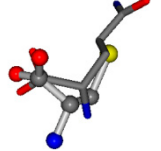
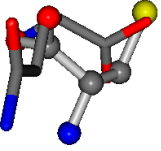
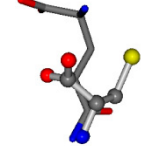
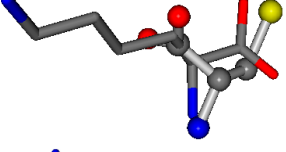
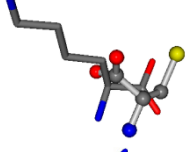
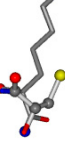
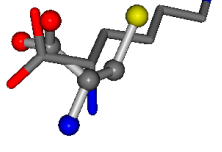
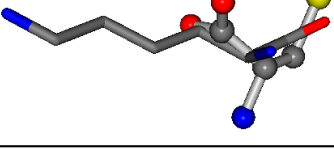
3D Views of Alignment	Aligned Structure and Index	TM-Score	Selected Atoms from 000750	$-2S_x$, $-2S_y$, and $-2S_z$ of the Reference Candidate	Selected Atoms from the Aligned Structure	$-2S_x$, $-2S_y$, and $-2S_z$ of the Aligned Candidate
	005961-155	0.55368	SOOCCC	-5.2465 -88.3648 -122.3962	COOCNC	-118.8959 -26.4831 -65.5527
	005961-179	0.5482	SOONCC	-28.5971 -38.2796 -135.5565	OCCNCC	-14.3175 -66.8735 -113.4675
	005961-230	0.59214	SOOCCC	-28.5971 -38.2796 -135.5565	COOCNC	-118.8959 -26.4831 -65.5527
	005961-239	0.55869	SOOCCC	-28.5971 -38.2796 -135.5565	OCNCOC	-118.8959 -65.5527 -26.4831
	005961-242	0.56355	SNCCC	-28.9822 -86.0507 -136.5352	CNCOC	-210.7718 -1.4071 -33.3867
	005962-1	0.43119	SONCCC	-37.2279 -107.1892 -159.5151	OCNCOC	-8.8452 -80.0543 -237.5683
	005962-2	0.39314	SONCCC	-31.7674 -35.7196 -105.9193	OCNCOC	-8.8452 -237.5683 -80.0543
	005962-3	0.41372	SONCCC	-37.2279 -107.1892 -159.5151	CNOCOC	-237.5683 -8.8452 -80.0543
	005962-15	0.44908	SOONCCC	-37.2279 -107.1892 -159.5151	COONCCC	-8.8452 -80.0543 -237.5683
	005962-18	0.40717	SOOCCC	-37.2279 -107.1892 -159.5151	ONCCCC	-237.5683 -80.0543 -8.8452

Table A2. Cont.

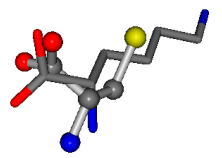
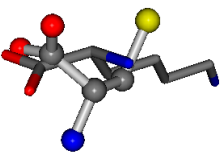
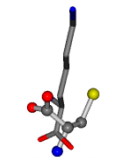
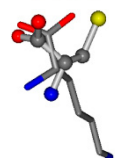
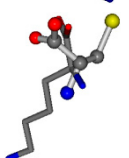
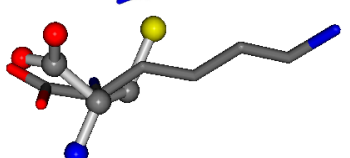
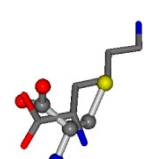
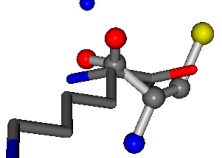
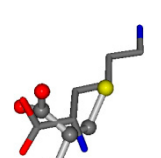
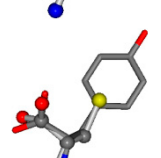
3D Views of Alignment	Aligned Structure and Index	TM-Score	Selected Atoms from 000750	$-2S_x$, $-2S_y$, and $-2S_z$ of the Reference Candidate	Selected Atoms from the Aligned Structure	$-2S_x$, $-2S_y$, and $-2S_z$ of the Aligned Candidate
	005962-23	0.44908	SOONCCC	-37.2279 -107.1892 -159.5151	COONCCC	-237.5683 -8.8452 -80.0543
	005962-25	0.4643	SOOCCC	-37.2279 -107.1892 -159.5151	COOCCC	-237.5683 -80.0543 -8.8452
	005962-30	0.40299	OONCC	-31.7674 -35.7196 -105.9193	CNOCC	-7.4698 -103.8043 -62.1387
	005962-32	0.39753	SONCCC	-31.7674 -35.7196 -105.9193	OONCCC	-103.8043 -62.1387 -7.4698
	005962-34	0.44778	OONCC	-31.7674 -35.7196 -105.9193	OONCC	-103.8043 -7.4698 -62.1387
	005962-39	0.41984	SOOCCC	-31.7674 -35.7196 -105.9193	COOCNC	-7.4698 -62.1387 -103.8043
	005962-40	0.46743	SONCCC	-31.7674 -35.7196 -105.9193	COOCNC	-7.4698 -62.1387 -103.8043
	005962-46	0.38057	SOOCCC	-31.7674 -35.7196 -105.9193	OCNCOC	-7.4698 -62.1387 -103.8043
	005962-48	0.46743	SONCCC	-31.7674 -35.7196 -105.9193	COOCNC	-103.8043 -7.4698 -62.1387
	006057-16	0.76753	SOONCCC	-37.2279 -107.1892 -159.5151	COONCCC	-173.9182 -101.9463 -23.1192

Table A2. Cont.

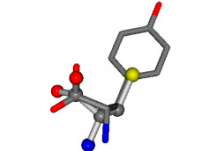
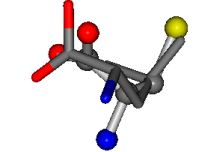
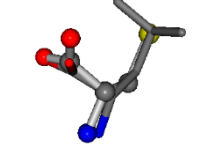
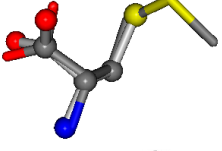
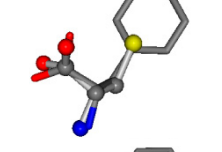
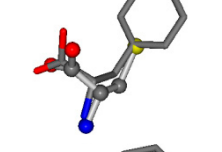
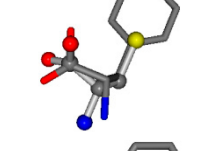
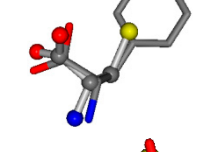
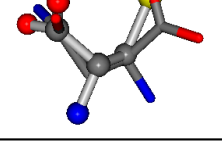
3D Views of Alignment	Aligned Structure and Index	TM-Score	Selected Atoms from 000750	$-2S_x$, $-2S_y$, and $-2S_z$ of the Reference Candidate	Selected Atoms from the Aligned Structure	$-2S_x$, $-2S_y$, and $-2S_z$ of the Aligned Candidate
	006057-144	0.62652	SOONCCC	-28.5971 -38.2796 -135.5565	COONCCC	-13.4258 -40.6418 -148.5831
	006106-16	0.54749	SOOCCC	-37.2279 -107.1892 -159.5151	COOCCC	-28.1552 -71.8562 -208.2835
	006106-83	0.68249	SOONCCC	-37.2279 -107.1892 -159.5151	COONCCC	-37.4924 -148.3439 -113.3827
	006137-18	0.8267	SOONCCC	-37.2279 -107.1892 -159.5151	COONCCC	-156.8033 -107.15 -27.0805
	006140-5	0.65026	SOONCCC	-11.1453 -70.4461 -121.9608	COONCCC	-9.3713 -53.8297 -141.0272
	006140-28	0.76831	SOONCCC	-37.2279 -107.1892 -159.5151	COONCCC	-173.9288 -101.9683 -23.0865
	006140-228	0.62808	SOONCCC	-28.5971 -38.2796 -135.5565	COONCCC	-108.7941 -87.3884 -5.489
	006140-256	0.62895	SOONCCC	-28.5971 -38.2796 -135.5565	COONCCC	-13.4284 -40.6224 -148.603
	006140-453	0.69151	SOONCCC	-31.8416 -89.3906 -126.7171	COONCCC	-148.4493 -83.8248 -16.8891
	006267-150	0.75426	SOOCCC	-28.5971 -38.2796 -135.5565	OONCCC	-114.7445 -56.4402 -32.1581

Table A2. Cont.

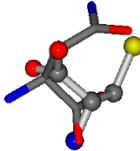
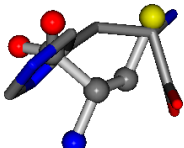
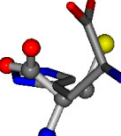
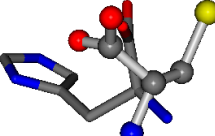
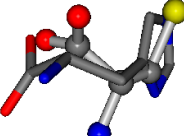
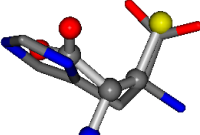
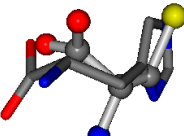
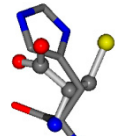
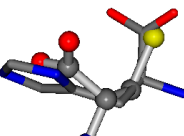
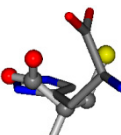
3D Views of Alignment	Aligned Structure and Index	TM-Score	Selected Atoms from 000750	$-2S_x$, $-2S_y$, and $-2S_z$ of the Reference Candidate	Selected Atoms from the Aligned Structure	$-2S_x$, $-2S_y$, and $-2S_z$ of the Aligned Candidate
	006267-270	0.64267	OONCCC	-30.6696 -83.1536 -110.9209	CNOCOC	-157.5302 -52.8112 -14.0738
	006274-11	0.52022	SOOCC	-30.6696 -83.1536 -110.9209	CCNCC	-29.2987 -34.082 -161.888
	006274-20	0.51619	OCCC	-37.2279 -107.1892 -159.5151	CCCN	-8.53 -238.2463 -49.0387
	006274-44	0.47052	OONCC	-31.7674 -35.7196 -105.9193	OONCC	-104.752 -19.0687 -49.267
	006274-75	0.48041	SOOCCC	-11.1453 -70.4461 -121.9608	CNOCCC	-27.4473 -30.9096 -145.1067
	006274-78	0.58417	SOOCCC	-11.1453 -70.4461 -121.9608	CNCCCC	-145.1067 -30.9096 -27.4473
	006274-83	0.48041	SOOCCC	-11.1453 -70.4461 -121.9608	CNOCCC	-145.1067 -27.4473 -30.9096
	006274-140	0.47356	SOONCC	-28.9822 -86.0507 -136.5352	NCOCCC	-7.9674 -210.2593 -33.7955
	006274-151	0.5215	SOOCCC	-28.9822 -86.0507 -136.5352	CNCCCC	-210.2593 -7.9674 -33.7955
	006274-170	0.48165	OCCC	-28.9822 -86.0507 -136.5352	CCCN	-6.8009 -203.291 -41.7099

Table A2. Cont.

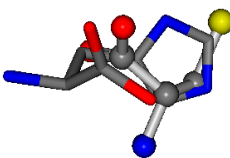
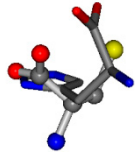
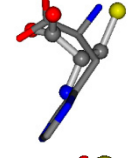
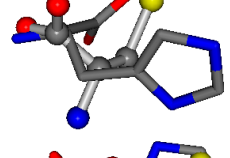
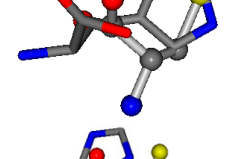
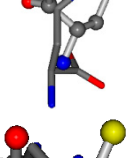
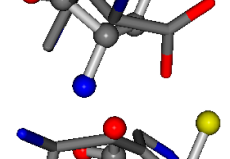
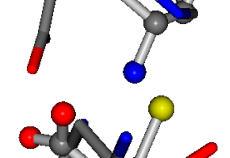
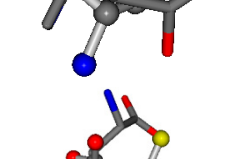
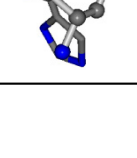
3D Views of Alignment	Aligned Structure and Index	TM-Score	Selected Atoms from 000750	$-2S_x$, $-2S_y$, and $-2S_z$ of the Reference Candidate	Selected Atoms from the Aligned Structure	$-2S_x$, $-2S_y$, and $-2S_z$ of the Aligned Candidate
	006274-175	0.48518	SOOCCC	-28.9822 -86.0507 -136.5352	CCCCNC	-6.8009 -41.7099 -203.291
	006274-184	0.48165	OCCC	-28.9822 -86.0507 -136.5352	CCCN	-41.7099 -6.8009 -203.291
	006274-188	0.47675	SOONCCC	-28.9822 -86.0507 -136.5352	NOOCCCC	-175.3227 -13.4702 -62.6855
	006274-195	0.54066	SOCCC	-28.9822 -86.0507 -136.5352	ONCCC	-13.4702 -175.3227 -62.6855
	006274-253	0.51888	SOOCCC	-28.9822 -86.0507 -136.5352	CCCCCC	-170.4509 -72.8278 -7.6721
	006274-266	0.49887	OONCC	-30.6696 -83.1536 -110.9209	NCCCC	-29.2987 -161.888 -34.082
	006274-270	0.47705	OONC	-30.6696 -83.1536 -110.9209	CNCC	-29.2987 -161.888 -34.082
	006274-275	0.4984	SOOCCC	-30.6696 -83.1536 -110.9209	NCCNCC	-29.2987 -34.082 -161.888
	006274-284	0.47705	OONC	-30.6696 -83.1536 -110.9209	CNCC	-34.082 -29.2987 -161.888
	006274-291	0.47128	SOONCC	-31.8416 -89.3906 -126.7171	OCNCCC	-9.7892 -202.8613 -35.0825

Table A2. Cont.

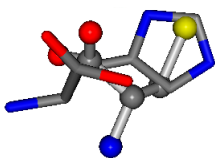
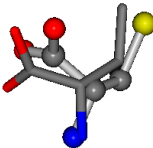
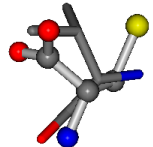
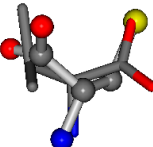
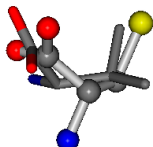
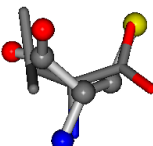
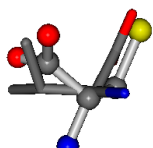
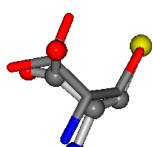
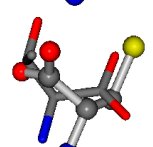
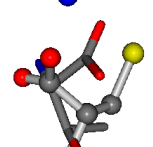
3D Views of Alignment	Aligned Structure and Index	TM-Score	Selected Atoms from 000750	$-2S_x$, $-2S_y$, and $-2S_z$ of the Reference Candidate	Selected Atoms from the Aligned Structure	$-2S_x$, $-2S_y$, and $-2S_z$ of the Aligned Candidate
	006274-303	0.47216	SOOCCC	-31.8416 -89.3906 -126.7171	CCCCCC	-202.8613 -35.0825 -9.7892
	006287-1	0.44763	SOONCCC	-37.2279 -107.1892 -159.5151	COONCCC	-28.463 -162.9622 -112.2806
	006287-10	0.50113	ONCCC	-37.2279 -107.1892 -159.5151	COCNC	-28.463 -112.2806 -162.9622
	006287-14	0.43465	SOONCCC	-37.2279 -107.1892 -159.5151	OCCNCCC	-28.463 -112.2806 -162.9622
	006287-20	0.43271	SOOCCC	-37.2279 -107.1892 -159.5151	COOCCC	-28.463 -112.2806 -162.9622
	006287-22	0.43465	SOONCCC	-37.2279 -107.1892 -159.5151	OCCNCCC	-162.9622 -28.463 -112.2806
	006287-24	0.46687	SOOCCC	-37.2279 -107.1892 -159.5151	OCCCCC	-162.9622 -112.2806 -28.463
	006288-1	0.48391	SOONCCC	-37.2279 -107.1892 -159.5151	OONCCC	-43.0635 -66.5743 -180.8565
	006288-3	0.45585	SOONCCC	-11.1453 -70.4461 -121.9608	OCCNOCC	-43.0635 -180.8565 -66.5743
	006288-6	0.45633	OONCCC	-37.2279 -107.1892 -159.5151	CNOCCC	-43.0635 -180.8565 -66.5743

Table A2. Cont.

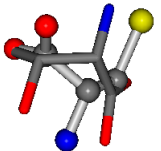
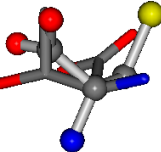
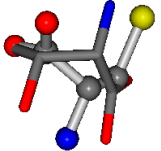
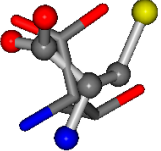
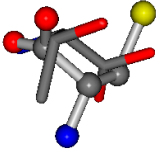
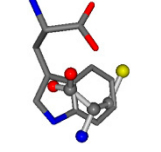
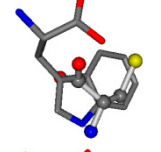
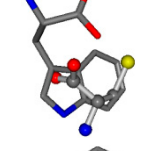
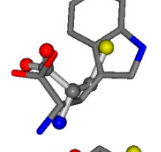
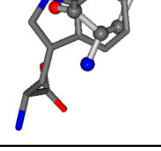
3D Views of Alignment	Aligned Structure and Index	TM-Score	Selected Atoms from 000750	$-2S_x$, $-2S_y$, and $-2S_z$ of the Reference Candidate	Selected Atoms from the Aligned Structure	$-2S_x$, $-2S_y$, and $-2S_z$ of the Aligned Candidate
	006288-13	0.51827	SONCCC	-37.2279 -107.1892 -159.5151	NCOCCC	-180.8565 -66.5743 -43.0635
	006288-26	0.5201	SOOCCC	-37.2279 -107.1892 -159.5151	OCOCCC	-180.8565 -66.5743 -43.0635
	006288-28	0.51827	SONCCC	-37.2279 -107.1892 -159.5151	NCOCCC	-8.4024 -103.7817 -61.1853
	006288-37	0.42733	SONCCC	-31.7674 -35.7196 -105.9193	OONCOC	-8.4024 -61.1853 -103.7817
	006288-72	0.42211	SOOCCC	-11.1453 -70.4461 -121.9608	OCNCOC	-29.1037 -62.1843 -111.9187
	006305-1	0.50837	SONCCC	-37.2279 -107.1892 -159.5151	CCCCCC	-1.9654 -82.3993 -214.7367
	006305-2	0.56881	SONCCC	-37.2279 -107.1892 -159.5151	CCNCCC	-3.6968 -75.0753 -224.1486
	006305-5	0.48382	SONCCC	-37.2279 -107.1892 -159.5151	CCNCCC	-2.4671 -82.2841 -211.504
	006305-9	0.54483	SOONCCC	-37.2279 -107.1892 -159.5151	COONCCC	-1.9654 -214.7367 -82.3993
	006305-23	0.47679	SONCCC	-37.2279 -107.1892 -159.5151	CNCCCC	-214.7367 -1.9654 -82.3993

Table A2. Cont.

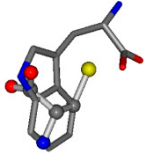
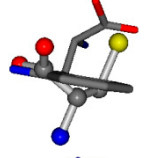
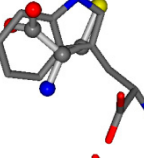
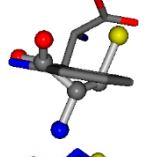
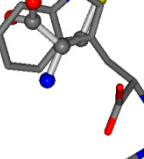
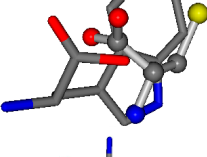
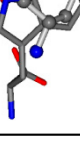
3D Views of Alignment	Aligned Structure and Index	TM-Score	Selected Atoms from 000750	$-2S_{x_r}$, $-2S_{y_r}$, and $-2S_{z_r}$ of the Reference Candidate	Selected Atoms from the Aligned Structure	$-2S_{x_r}$, $-2S_{y_r}$, and $-2S_{z_r}$ of the Aligned Candidate
	006305-35	0.51784	SONCCC	-37.2279 -107.1892 -159.5151	CNCCCC	-224.1486 -3.6968 -75.0753
	006305-36	0.50682	OOCCC	-37.2279 -107.1892 -159.5151	CNCCC	-75.0753 -224.1486 -3.6968
	006305-44	0.51678	SOONCCC	-37.2279 -107.1892 -159.5151	CCCCCCC	-224.1486 -75.0753 -3.6968
	006305-49	0.50682	OOCCC	-37.2279 -107.1892 -159.5151	CNCCC	-75.0753 -3.6968 -224.1486
	006305-59	0.51678	SOONCCC	-37.2279 -107.1892 -159.5151	CCCCCCC	-1.8573 -208.8667 -86.2881
	006305-60	0.53173	SONCCC	-37.2279 -107.1892 -159.5151	CNCCCC	-208.8667 -1.8573 -86.2881
	006305-88	0.49077	SONCCC	-37.2279 -107.1892 -159.5151	NCCCCC	-0.5256 -221.8958 -77.1639
	006305-93	0.4984	SONCCC	-37.2279 -107.1892 -159.5151	CCCCCC	-0.5256 -77.1639 -221.8958
	006305-97	0.56351	SOONCCC	-37.2279 -107.1892 -159.5151	CCCCCNC	-0.5256 -77.1639 -221.8958
	006305-98	0.56197	SONCCC	-37.2279 -107.1892 -159.5151	CNCCCC	-221.8958 -0.5256 -77.1639

Table A2. Cont.

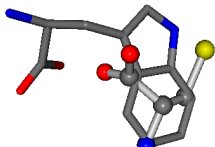
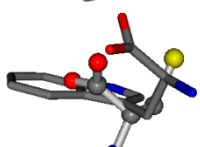
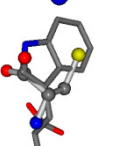
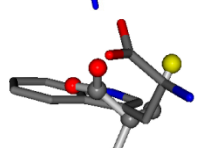
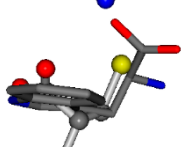
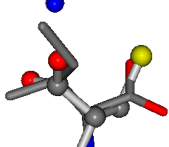
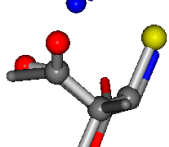
3D Views of Alignment	Aligned Structure and Index	TM-Score	Selected Atoms from 000750	$-2S_x$, $-2S_y$, and $-2S_z$ of the Reference Candidate	Selected Atoms from the Aligned Structure	$-2S_x$, $-2S_y$, and $-2S_z$ of the Aligned Candidate
	006305-105	0.56351	SOONCCC	-37.2279 -107.1892 -159.5151	CCCCNC	-221.8958 -0.5256 -77.1639
	006305-110	0.56356	SONCCC	-37.2279 -107.1892 -159.5151	CNCCCC	-211.504 -2.4671 -82.2841
	006305-138	0.50276	SOONCCC	-37.2279 -107.1892 -159.5151	NCOCCCC	-1.4469 -210.87 -83.7564
	006305-163	0.59418	SONCCC	-37.2279 -107.1892 -159.5151	CCCCNC	-0.0058 -216.4546 -93.9712
	006305-186	0.49257	OOCCC	-37.2279 -107.1892 -159.5151	CCCCC	-48.5216 -239.5349 -13.6686
	006305-188	0.48355	SONCCC	-37.2279 -107.1892 -159.5151	CNCCCC	-13.6686 -239.5349 -48.5216
	006305-199	0.49257	OOCCC	-37.2279 -107.1892 -159.5151	CCCCC	-48.5216 -13.6686 -239.5349
	006305-200	0.47666	SOOCCC	-37.2279 -107.1892 -159.5151	CCNCCC	-239.5349 -48.5216 -13.6686
	006306-26	0.59343	SOONCCC	-37.2279 -107.1892 -159.5151	OCCNCCC	-187.941 -40.4448 -79.4912
	006306-106	0.68164	SOCCC	-5.2465 -88.3648 -122.3962	NCCCC	-20.4327 -39.2382 -155.9536

Table A2. Cont.

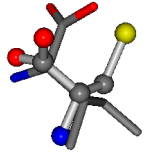
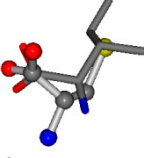
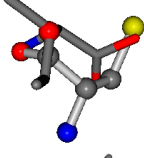
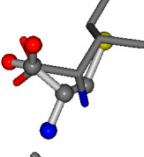
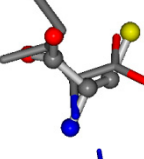
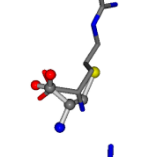
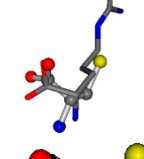
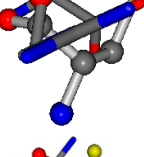
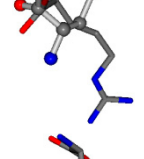
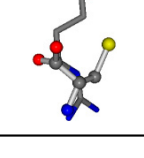
3D Views of Alignment	Aligned Structure and Index	TM-Score	Selected Atoms from 000750	$-2S_{x_r}$, $-2S_{y_r}$, and $-2S_{z_r}$ of the Reference Candidate	Selected Atoms from the Aligned Structure	$-2S_{x_r}$, $-2S_{y_r}$, and $-2S_{z_r}$ of the Aligned Candidate
	006306-141	0.57733	OONCCC	-5.2465 -88.3648 -122.3962	CNCCCC	-18.3555 -160.9526 -36.9999
	006306-175	0.54571	SOOCCC	-28.5971 -38.2796 -135.5565	COOCNC	-28.3736 -66.0039 -109.0218
	006306-181	0.54665	SOOCCC	-28.5971 -38.2796 -135.5565	OCNCOC	-28.3736 -66.0039 -109.0218
	006306-183	0.54571	SOOCCC	-28.5971 -38.2796 -135.5565	COOCNC	-109.0218 -28.3736 -66.0039
	006306-226	0.56045	SOONCCC	-28.9822 -86.0507 -136.5352	OCCNCCC	-152.9247 -33.7788 -64.0308
	006322-2	0.55916	SOOCCC	-28.5971 -38.2796 -135.5565	COOCNC	-27.3384 -62.6263 -111.6846
	006322-19	0.4956	SOONCCC	-37.2279 -107.1892 -159.5151	COONCCC	-158.5429 -38.7577 -80.7785
	006322-42	0.5614	SOOCCC	-28.5971 -38.2796 -135.5565	OCNCOC	-27.3384 -62.6263 -111.6846
	006322-44	0.46472	SOOCCC	-28.5971 -38.2796 -135.5565	NOOCCC	-111.6846 -27.3384 -62.6263
	006322-56	0.49042	ONCCC	-28.9822 -86.0507 -136.5352	CNCNC	-221.7222 -6.933 -23.1061

Table A2. Cont.

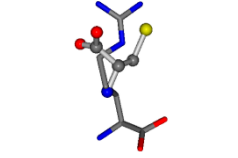
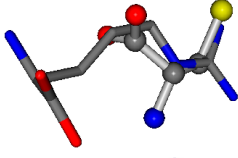
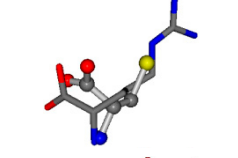
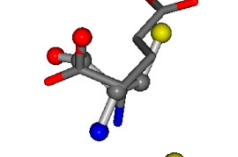
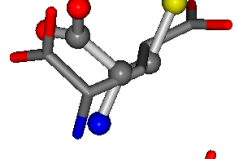
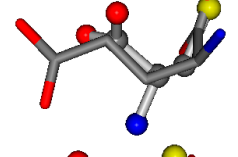
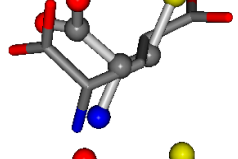
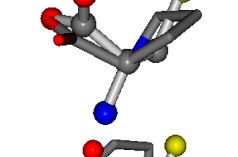
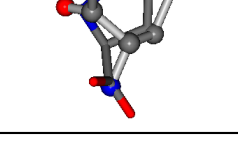
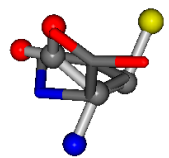
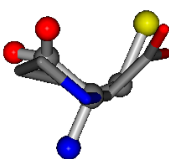
3D Views of Alignment	Aligned Structure and Index	TM-Score	Selected Atoms from 000750	$-2S_{x_r}$, $-2S_{y_r}$, and $-2S_{z_r}$ of the Reference Candidate	Selected Atoms from the Aligned Structure	$-2S_{x_r}$, $-2S_{y_r}$, and $-2S_{z_r}$ of the Aligned Candidate
	006322-60	0.4524	SNCC	-28.9822 -86.0507 -136.5352	NCNC	-221.7222 -23.1061 -6.933
	006322-69	0.51145	SOOCCC	-28.9822 -86.0507 -136.5352	NCCNCC	-221.7222 -6.933 -23.1061
	006322-90	0.4613	SOONCCC	-28.9822 -86.0507 -136.5352	COCNCCC	-204.5901 -27.1111 -18.7144
	033032-13	0.56115	SOONCCC	-37.2279 -107.1892 -159.5151	COONCCC	-157.6594 -87.1404 -38.0414
	033032-66	0.45269	SOONCCC	-31.8416 -89.3906 -126.7171	COONCCC	-12.4748 -35.4453 -199.7397
	033032-69	0.51437	SOCCC	-31.8416 -89.3906 -126.7171	OCCOC	-199.7397 -35.4453 -12.4748
	033032-74	0.45269	SOONCCC	-31.8416 -89.3906 -126.7171	COONCCC	-199.7397 -12.4748 -35.4453
	145742-21	0.59575	SOOCCC	-37.2279 -107.1892 -159.5151	COOCNC	-24.7574 -57.3704 -227.05
	145742-28	0.53132	SONCCC	-11.1453 -70.4461 -121.9608	CCCCCN	-145.192 -12.4766 -45.8437

Table A2. Cont.

3D Views of Alignment	Aligned Structure and Index	TM-Score	Selected Atoms from 000750	$-2S_x$, $-2S_y$, and $-2S_z$ of the Reference Candidate	Selected Atoms from the Aligned Structure	$-2S_x$, $-2S_y$, and $-2S_z$ of the Aligned Candidate
	145742-29	0.52833	OONCCC	-11.1453 -70.4461 -121.9608	OCNCCC	-45.8437 -145.192 -12.4766
	145742-43	0.48734	SOCCC	-11.1453 -70.4461 -121.9608	CCNCC	-145.192 -45.8437 -12.4766

References

- Dong, R.; Pan, S.; Peng, Z.; Zhang, Y.; Yang, J. MTM-ALIGN: A server for fast protein structure database search and multiple protein structure alignment. *Nucleic Acids Res.* **2018**, *46*, 380–386. [\[CrossRef\]](#)
- Zhao, C.; Sacan, A. UniAlign: Protein structure alignment meets evolution. *Bioinformatics* **2015**, *31*, 3139–3146. [\[CrossRef\]](#)
- Hasegawa, H.; Holm, L. Advances and pitfalls of protein structural alignment. *Curr. Opin. Struct. Biol.* **2009**, *19*, 341–348. [\[CrossRef\]](#) [\[PubMed\]](#)
- Kolodny, R.; Koehl, P.; Levitt, M. Comprehensive evaluation of protein structure alignment methods: Scoring by geometric measures. *J. Mol. Biol.* **2005**, *346*, 1173–1188. [\[CrossRef\]](#) [\[PubMed\]](#)
- Terashi, G.; Takeda-Shitaka, M. CAB-Align: A flexible protein structure alignment method based on the residue-residue contact area. *PLoS ONE* **2015**, *10*, e0141440. [\[CrossRef\]](#) [\[PubMed\]](#)
- Akdel, M.; Durairaj, J.; de Ridder, D.; van Dijk, A.D.J. Caretta-A multiple protein structure alignment and feature extraction suite. *comput. struct. Biotechnol. J.* **2020**, *18*, 981–992. [\[CrossRef\]](#)
- Holm, L. Using dali for protein structure comparison. In *Structural Bioinformatics*; Gáspári, Z., Ed.; Methods in Molecular Biology; Springer: New York, NY, USA, 2020; Volume 2112, pp. 29–42; ISBN 978-1-07-160269-0.
- Hu, J.; Liu, Z.; Yu, D.-J.; Zhang, Y. LS-Align: An atom-level, flexible ligand structural alignment algorithm for high-throughput virtual screening. *Bioinformatics* **2018**, *34*, 2209–2218. [\[CrossRef\]](#) [\[PubMed\]](#)
- Menke, M.; Berger, B.; Cowen, L. Matt: Local flexibility aids protein multiple structure alignment. *PLoS Comput. Biol.* **2008**, *4*, 88–99. [\[CrossRef\]](#) [\[PubMed\]](#)
- Zhang, Y. TM-Align: A protein structure alignment algorithm based on the tm-Score. *Nucleic Acids Res.* **2005**, *33*, 2302–2309. [\[CrossRef\]](#)
- Chen, W.; Yao, C.; Guo, Y.; Wang, Y.; Xue, Z. PmTM-Align: Scalable pairwise and multiple structure alignment with apache spark and openmp. *BMC Bioinform.* **2020**, *21*, 426. [\[CrossRef\]](#)
- Shegay, M.V.; Suplatov, D.A.; Popova, N.N.; Švedas, V.K.; Voevodin, V.V. ParMATT: Parallel multiple alignment of protein 3D-structures with translations and twists for distributed-memory systems. *Bioinformatics* **2019**, *35*, 4456–4458. [\[CrossRef\]](#) [\[PubMed\]](#)
- Dong, R.; Peng, Z.; Zhang, Y.; Yang, J. MTM-Align: An algorithm for fast and accurate multiple protein structure alignment. *Bioinformatics* **2018**, *34*, 1719–1725. [\[CrossRef\]](#)
- Holm, L. DALI and the persistence of protein shape. *Protein Sci.* **2020**, *29*, 128–140. [\[CrossRef\]](#) [\[PubMed\]](#)
- Jäntschi, L. The eigenproblem translated for alignment of molecules. *Symmetry* **2019**, *11*, 1027. [\[CrossRef\]](#)
- Huang, J.; Zhang, M.; Ma, J.; Liu, X.; Kobbelt, L.; Bao, H. Spectral quadrangulation with orientation and alignment control. In Proceedings of the ACM SIGGRAPH Asia 2008 Papers, Singapore, 10–13 December 2008; Hart, J.C., Ed.; Association for Computing Machinery: New York, NY, USA, 2008; Volume 147, pp. 1–9.
- Norrdine, A.; Kasmi, Z.; Ahmed, K.; Motzko, C.; Schiller, J. MQTT-Based Surveillance System of IoT Using UWB Real Time Location System. In Proceedings of the 2020 International Conferences on Internet of Things (iThings) and IEEE Green Computing and Communications (GreenCom) and IEEE Cyber, Physical and Social Computing (CPSCom) and IEEE Smart Data (SmartData) and IEEE Congress on Cybermatics (Cybermatics), Rhodes, Greece, 2–6 November 2020; IEEE: Piscataway, NJ, USA, 2020; pp. 216–221. [\[CrossRef\]](#)
- Xu, Z.; Huang, X.; Jimenez, F.; Deng, Y. A new record of graph enumeration enabled by parallel processing. *Mathematics* **2019**, *7*, 1214. [\[CrossRef\]](#)

19. Medina, L.; Nina, H.; Trigo, M. On distance signless laplacian spectral radius and distance signless laplacian energy. *Mathematics* **2020**, *8*, 792. [[CrossRef](#)]
20. Hayat, S.; Khan, S.; Khan, A.; Liu, J.-B. Valency-based molecular descriptors for measuring the π -electronic energy of lower polycyclic aromatic hydrocarbons. *Polycycl. Aromat. Compd.* **2020**, *1*, 1–17. [[CrossRef](#)]
21. Hayat, S.; Khan, S. Quality testing of spectrum-based valency descriptors for polycyclic aromatic hydrocarbons with applications. *J. Mol. Struct.* **2021**, *1228*, 129789. [[CrossRef](#)]
22. Tomescu, M.A.; Jäntschi, L.; Rotaru, D.I. Figures of graph partitioning by counting, sequence and layer matrices. *Mathematics* **2021**, *9*, 1419. [[CrossRef](#)]
23. Jukic, S.; Saracevic, M.; Subasi, A.; Kevric, J. Comparison of ensemble machine learning methods for automated classification of focal and non-focal epileptic EEG signals. *Mathematics* **2020**, *8*, 1481. [[CrossRef](#)]
24. Zhang, C.; Pei, D. Generalized bertrand curves in minkowski 3-space. *Mathematics* **2020**, *8*, 2199. [[CrossRef](#)]
25. Tirkolaee, E.B.; Dashtian, Z.; Weber, G.-W.; Tomaskova, H.; Soltani, M.; Mousavi, N.S. An integrated decision-making approach for green supplier selection in an agri-food supply chain: Threshold of robustness worthiness. *Mathematics* **2021**, *9*, 1304. [[CrossRef](#)]
26. Wei, Y.; Zheng, Y.; Jiang, Z.; Shon, S. A study of determinants and inverses for periodic tridiagonal toeplitz matrices with perturbed corners involving mersenne numbers. *Mathematics* **2019**, *7*, 893. [[CrossRef](#)]
27. Gasiński, L.; Papageorgiou, N.S. Resonant anisotropic (p,q)-equations. *Mathematics* **2020**, *8*, 1332. [[CrossRef](#)]
28. Moaaz, O.; Furuichi, S.; Muhib, A. New comparison theorems for the nth order neutral differential equations with delay inequalities. *Mathematics* **2020**, *8*, 454. [[CrossRef](#)]
29. Kamran, K.; Shah, Z.; Kumam, P.; Alreshidi, N.A. A meshless method based on the laplace transform for the 2D multi-term time fractional partial integro-differential equation. *Mathematics* **2020**, *8*, 1972. [[CrossRef](#)]
30. Sharma, J.R.; Kumar, S.; Jäntschi, L. On a class of optimal fourth order multiple root solvers without using derivatives. *Symmetry* **2019**, *11*, 1452. [[CrossRef](#)]
31. Kumar, D.; Sharma, J.R.; Jäntschi, L. A novel family of efficient weighted-newton multiple root iterations. *Symmetry* **2020**, *12*, 1494. [[CrossRef](#)]